AD-A111 273 SAN DIEGO STATE UNIV CA DEPT OF AEROSPACE ENGINEERIN--ETC F/G 11/3
COMPLIANT-COATING-FLUID INTERACTION: COATING SHEAR WAVES IN STA--ETC(U)
FEB 82 M PIERUCCI, P A BAXLEY N00014-81-K-0424
UNCLASSIFIED AE/EM-TR-82-03 NL

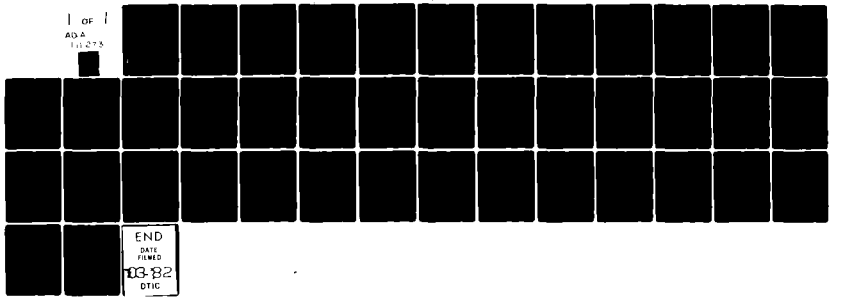

12

AE&EM TR-82-03

COMPLIANT-COATING-FLUID INTERACTION: COATING SHEAR WAVES IN STATIONARY FLUID

Mauro Pierucci
Paul A. Baxley

February 1982

Research Sponsored by Office of Naval Research under Contract N00014-81-K-0424

Approved for Public Release – Distribution Unlimited

SAN DIEGO STATE UNIVERSITY
College of Engineering
Department of Aerospace Engineering
and Engineering Mechanics
San Diego, CA 92182-0183
(714) 265-6074

Unclassified

SECURITY CLASSIFICATION OF THIS PAGE (When Data Entered)

REPORT DOCUMENTATION PAGE		READ INSTRUCTIONS BEFORE COMPLETING FORM
1. REPORT NUMBER AE&EM TR 82-03	2. GOVT ACCESSION NO. AD-A111 273	3. RECIPIENT'S CATALOG NUMBER
4. TITLE (and Subtitle) Compliant Coating-Fluid Interaction:Coating Shear Waves in Stationary Fluid		5. TYPE OF REPORT & PERIOD COVERED Final March 1981-Feb. 1982
		6. PERFORMING ORG. REPORT NUMBER AE&EM TR 82-03
7. AUTHOR(s) Mauro Pierucci Paul A. Baxley		8. CONTRACT OR GRANT NUMBER(s) N00014-81-K-0424
9. PERFORMING ORGANIZATION NAME AND ADDRESS Aerospace Engineering and Engineering Mechanics San Diego State University San Diego, CA 92182		10. PROGRAM ELEMENT, PROJECT, TASK AREA & WORK UNIT NUMBERS ONR 062-693
11. CONTROLLING OFFICE NAME AND ADDRESS Department of the Navy Office of Naval Research-Fluid Dynamics Division Arlington, Virginia 22217		12. REPORT DATE February 1982 13. NUMBER OF PAGES 30 + 8 Appendix Pages
14. MONITORING AGENCY NAME & ADDRESS(if different from Controlling Office)		15. SECURITY CLASS.(of this report) Unclassified 15a. DECLASSIFICATION/DOWNGRADING SCHEDULE

16. DISTRIBUTION STATEMENT (of this Report)

Approved for public release; distribution unlimited.

17. DISTRIBUTION STATEMENT (of the abstract entered in Block 20, if different from Report)

18. SUPPLEMENTARY NOTES

19. KEY WORDS (Continue on reverse side if necessary and identify by block number)

Shear Waves; Fluid-Structure Interaction; Compliant Coating Transition layer; non-homogeneous layer; viscoelastic layer.

20. ABSTRACT (Continue on reverse side if necessary and identify by block number)

The objective of this work is to study the transfer of energy between an elastic solid coating, a viscoelastic non-homogeneous layer and the surrounding viscous fluid. The particle displacements and stress distributions in the solid and the fluid are analyzed. The motion at the lower boundary of the elastic solid is assumed given. The effect of coating properties, transition layer thickness and frequency are obtained.

DD FORM 1 JAN 73 1473 EDITION OF 1 NOV 65 IS OBSOLETE
S/N 0102-LF-014-6601

Unclassified

SECURITY CLASSIFICATION OF THIS PAGE (When Data Entered)

TABLE OF CONTENTS

ABSTRACT

The objective of this work is to study the transfer of energy between an elastic solid coating, a viscoelastic non-homogeneous layer and the surrounding viscous fluid. The particle displacements and stress distributions in the solid and the fluid are analyzed. The motion at the lower boundary of the elastic solid is assumed given. The effect of coating properties, transition layer thickness and frequency are obtained.

I - INTRODUCTION

The drag of a flow field over a surface will be reduced if the energy content of the fluid can be decreased. The design of a drag reducing compliant coating thus requires a mechanism whereby the coating interacts with the fluid in such manner as to either absorb or cancel the fluid disturbances. The accomplishment of this goal requires an understanding of the transfer mechanism between the solid and the fluid.

The transfer of energy between a solid and a fluid is accomplished by the continuity of particle displacement and stresses across the interface[1]. The presence of a viscoelastic non-homogeneous layer interposed between a solid and a fluid (Fig. 1) with properties varying from that of the solid to that of the fluid at the two extremes obscures the actual identity of the interface and of the boundary conditions.

Many different reasons exist for justifying the interest in the analysis of a thin viscoelastic non-homogeneous transition layer between a coating and the surrounding fluid. Kramer[2] in some of the early compliant coating work applied a thin layer of paint on the rubber surface of the coating. From a physical point of view, this transition layer can "bridge the gap" between the solid and the fluid in a more gradual manner and this may alter the energy transfer between the two media. When a compliant surface is exposed to a turbulent flow field, the surface will experience forces which will vary randomly in both the space and the time domain. The resulting surface motion will be composed of random modes superimposed upon some form of discrete motion. This complex motion will cause the classical wall boundary condition to be applied at a mean surface location which may vary as a function of both time and space. The set of interface boundary conditions may then be modelled by a system with the classical wall boundary conditions being satisfied along a layer whose thickness is equivalent to the crest to trough distance of the mean motion (Fig. 1).

Two different modes of energy transfer between a compliant coating and the surrounding fluid exist: shear and longitudinal waves. This report restricts its attention to shear waves only. For the sake of simplicity, the motion will be assumed to be one-dimensional (Fig. 2) and wall conditions prescribed at the lower boundary of the solid.

II. ANALYSIS

II-1 Derivation of Governing Equations

Consider a plane strain problem with no variations in the z direction (Fig. 2). The general equations of motion valid for a general medium are[3]:

$$\rho \frac{Dv_1}{Dt} = \frac{\partial \tau_{11}}{\partial x} + \frac{\partial \tau_{12}}{\partial y} \quad , \tag{1}$$

$$\rho \frac{Dv_2}{Dt} = \frac{\partial \tau_{21}}{\partial x} + \frac{\partial \tau_{22}}{\partial y} \quad , \tag{2}$$

$$\frac{D\rho}{Dt} + \rho \left(\frac{\partial v_1}{\partial x} + \frac{\partial v_2}{\partial y}\right) = 0 \quad , \tag{3}$$

where v_1 and v_2 are the velocities in the x and the y direction respectively and $\frac{D}{Dt}$ is the material derivative given by

$$\frac{D}{Dt} = \frac{\partial}{\partial t} + v_1 \frac{\partial}{\partial x} + v_2 \frac{\partial}{\partial y} \quad . \tag{4}$$

The stresses are given by

$$\tau_{11}\Big|_{solid} = \frac{2G}{1-2\nu}\left[(1-\nu)\frac{\partial u_1}{\partial x} + \nu \frac{\partial u_2}{\partial y}\right] \quad , \tag{5}$$

$$\tau_{11}\Big|_{fluid} = -p + \mu\left[\frac{4}{3}\frac{\partial v_1}{\partial x} - \frac{2}{3}\frac{\partial v_2}{\partial y}\right] \quad , \tag{6}$$

$$\tau_{12}\Big|_{solid} = G\left[\frac{\partial u_1}{\partial y} + \frac{\partial u_2}{\partial x}\right] \quad , \tag{7}$$

$$\tau_{12}\Big|_{fluid} = \mu\left[\frac{\partial v_1}{\partial y} + \frac{\partial v_2}{\partial x}\right] \quad , \tag{8}$$

$$\tau_{22}\Big|_{solid} = \frac{2G}{1-2\nu}\left[\nu \frac{\partial u_1}{\partial x} + (1-\nu)\frac{\partial u_2}{\partial y}\right] , \tag{9}$$

$$\tau_{22}\Big|_{fluid} = -p + \mu\left[-\frac{2}{3}\frac{\partial v_1}{\partial x} + \frac{4}{3}\frac{\partial v_2}{\partial y}\right] . \tag{10}$$

For a one-dimensional (no variations in the x direction) steady state ($\exp(-i\omega t)$) system, the governing equations simplify to:

$$\rho\left[v_2 \frac{dv_1}{dy} - i\omega v_1\right] = \frac{d\tau_{12}}{dy} \quad , \tag{11}$$

$$\rho\left[v_2 \frac{dv_2}{dy} - i\omega v_2\right] = \frac{d\tau_{22}}{dy} \quad , \tag{12}$$

$$\frac{d}{dy}(\rho v_2) - i\omega\rho = 0 \quad , \tag{13}$$

with

$$\tau_{12}\Big|_{solid} = G\frac{du_1}{dy} \quad , \tag{14}$$

$$\tau_{12}\Big|_{fluid} = \mu \frac{dv_1}{dy} \quad , \tag{15}$$

$$\tau_{22}\Big|_{solid} = \frac{2G(1-\nu)}{1-2\nu} \frac{du_2}{dy} \quad , \tag{16}$$

$$\tau_{22}\Big|_{fluid} = -p + \frac{4}{3}\mu\frac{dv_2}{dy} \quad . \tag{17}$$

If only shear modes are considered, then $v_2 = 0$; the system of differential equations is reduced to one,

$$\frac{d\tau_{12}}{dy} + i\rho\omega v_1 = 0 \quad , \tag{18}$$

where τ_{12} is given by either Eq. (14) or Eq. (15). The stress-strain relationships simplify for a fluid with zero mean flow velocity and with steady-state disturbances given by

$$u_1 = u_1 \exp(-i\omega t) \quad . \tag{19}$$

The stress-strain relationships for the solid and the fluid become

$$\tau_s = G \frac{du_1}{dy} \quad , \tag{20}$$

$$\tau_f = -i\omega\mu \frac{du_1}{dy} \quad . \tag{21}$$

Fig. 3 shows the magnitude of the stress-strain coefficient as a function of axial distance. In a typical solid-fluid system, the magnitude of the coefficient jumps from a value of G at the solid to a magnitude of $i\mu\omega$ in the fluid. The lowest values of the shear modulus for a very soft plastisol is about 10^4 N/m^2. For water at 10^4 Hz the value of $i\mu\omega$ is about 60 N/m^2. For more rigid surfaces and for lower frequencies, the difference between the value of G and $i\mu\omega$ increases.

In the presence of a transition layer the change can occur over a finite thickness. Introducing a generalized stress-strain relationship will allow one to combine Eqs. (20) and (21) into a single equation. This new unified approach leads to

$$\tau = K \frac{du_1}{dy} \quad , \tag{22}$$

where K is equal to G within the coating material, and is equal to $-i\mu\omega$ in the fluid; within the transition layer K takes on intermediate complex values. The governing differential equation then reduces to:

$$\frac{d}{dy}\left[K(y) \frac{du_1}{dy}\right] + \rho\omega^2 u_1 = 0 \quad . \tag{23}$$

For the particular case of interest in this study, where the interface region between the elastic solid and the fluid is assumed to be a non-homogeneous viscoelastic layer, the value of K(y) is assumed to be given by

$$K(y) = -i\mu\omega + \left[G + i\mu\omega\right] \exp(-y/\ell)^n \quad , \tag{24}$$

where ℓ is the thickness of the compliant coating and n is a parameter inversely proportional to the thickness of the transition layer. Note that for $y \ll \ell$ one recovers the shear modulus of the solid while for $y \gg \ell$ one obtains the fluid viscosity relationship. For simplicity it is assumed that the solid and the fluid have equal densities. The value of K(y) is non-dimensionalized with respect to G, thus

$$\frac{d}{dy}\left(H \frac{du_1}{dy}\right) + (\Gamma^2 R)\, u_1 = 0 \quad , \tag{25}$$

where

$$H(y) = -iR + (1 + iR) \exp(-y/\ell)^n \quad . \tag{26}$$

The value of R is defined to be the ratio of $i\mu\omega$ to G. The shear wave speed in a solid is given by

$$c_s^2 = G/\rho \quad , \tag{27}$$

while in a fluid the wave speed of the shear waves is given by

$$c_f^2 = \mu\omega/\rho \tag{28}$$

The value of R can then be written as the ratio of the two speeds

$$R = (c_f/c_s)^2 = (\lambda_f/\lambda_s)^2 \quad . \tag{29}$$

Fig. 4 shows the variation of the magnitude of H as a function of y/ℓ for different values of the layer thickness parameter n. Note that, in the limit as $n \to \infty$, the classical no-transition layer configuration is recovered.

The values of distance y and displacement u_1 have been non-dimensionalized with respect to the coating thickness ℓ and the magnitude of wall displacement respectively. Eq. (25) together with the proper boundary conditions represent the equation to be studied in this report. The boundary conditions of the problem are split; one condition is at the lower boundary of the coating while the other is the radiation condition at large distances from the surfaces. The inner boundary of the coating can move by imposing either a displacement or a force. The split boundary conditions then become

$$u_1(0) = 1 \quad ,$$

$$\lim_{y\to\infty} u_1(y) = C \exp\left[-(1+i)\,\Gamma y/(\sqrt{2}\ell)\right] \quad , \tag{30}$$

or

$$\left.\frac{du_1}{dy}\right|_{y=0} = 1 \quad ,$$

$$\lim_{y\to\infty} u_1(y) = C \exp\left[-(1+i)\,\Gamma y/(\sqrt{2}\ell)\right] \quad . \tag{31}$$

Boundary conditions as represented by Eq. (30) will give displacement-driven solutions while conditions of Eq. (31) will give force-driven solutions. Note that since the stress-strain coefficients have been non-dimensionalized with respect to G, the stress at the lower boundary is equal to the derivative of the particle displacement.

II-2 Numerical Solution

The solution to the problem considered in this report requires the numerical integration of Eq. (25)

$$\frac{d}{dy}\left(H \frac{du_1}{dy}\right) + (\Gamma^2 R)\, u_1 = 0 \quad . \tag{25-a}$$

The boundary conditions for the displacement-driven case are Eq. (30)

$$u_1(0) = 1 \quad ,$$

$$\lim_{y\to\infty} u_1(y) = C \exp\left[-(1+i)\Gamma y/(\sqrt{2}\ell)\right] \quad . \tag{30-a}$$

Eq. (25-a) was solved numerically by the Runge-Kutta technique. Values of slopes of displacements at y=0 were iterated until the far-field boundary condition, Eq. (30-a), was satisfied. For most cases of interest this procedure required 5 to 7 iterations. The iterations were performed by studying the sensitivity of the assumed slope at the wall (note that the values of the displacements and slopes are complex) upon the far-field radiation condition.

The values of the parameters Γ and R can be re-written in terms of length ratios as

$$\Gamma = 2\pi(\ell/\lambda_f) \quad , \tag{32}$$

$$R = (\lambda_f/\lambda_s)^2 \quad . \tag{33}$$

The range of values of Γ and R for different coating materials immersed in water are shown in Table 1.

C_s (m/sec)	R	ℓ (mm)	Γ
2500	$10^{-12}f$	100	$250\sqrt{f}$
250	$10^{-10}f$	10	$25\sqrt{f}$
25	$10^{-8}f$	1	$2.5\sqrt{f}$
2.5	$10^{-6}f$	0.1	$0.25\sqrt{f}$

Table 1- Values Γ and R for different coatings.

II-3 Modified Stokes Second Problem (MSSP)

In the limit as both the transition layer and the elastic solid layer thicknesses go to zero (i.e. $n\to\infty$ and $\ell\to 0$), one will obtain the classical Stokes second problem[4]. Stokes second problem corresponds to the propagation of shear disturbances in a viscous fluid produced by an oscillating plane wall. For a zero-thickness transition ($n\to\infty$) but a finite-thickness elastic solid one obtains the modified Stokes second problem (MSSP). In the MSSP, instead of driving the viscous fluid with a given displacement oscillation, the lower boundary of the solid is forced by the same function. The displacement on the lower boundary causes shear waves to be transmitted first through the elastic medium, then into the fluid. The fluid-structure coupling occurs at the solid-fluid interface where continuity of displacement and stresses are required.

The equations of motion representing the MSSP are

$$\rho \frac{\partial^2 u_1}{\partial t^2} = \frac{\partial \tau_1}{\partial y} \qquad 0 \le y \le \ell \quad , \tag{34}$$

$$\rho \frac{\partial^2 u_1}{\partial t^2} = \frac{\partial \tau_1}{\partial y} \qquad y \ge \ell \quad , \tag{35}$$

where the solid and the fluid stresses are related to the particle displacement u_1 by

$$\tau_1 = G \frac{\partial u_1}{\partial y} \qquad 0 \le y \le \ell \quad , \tag{36}$$

$$\tau_1 = \mu \frac{\partial}{\partial y} \left(\frac{\partial u_1}{\partial t}\right) \qquad y \ge \ell \quad . \tag{37}$$

The boundary and the interface boundary conditions are given by

$$u_1(0) = 1 \exp(-i\omega t) \quad , \tag{38}$$

$$u_1(\ell)\Big|_{\text{solid}} = u_1(\ell)\Big|_{\text{fluid}} \quad , \tag{39}$$

$$\tau_1(\ell)\Big|_{\text{solid}} = \tau_1(\ell)\Big|_{\text{fluid}} \quad . \tag{40}$$

The solution to Eqs. 34-35 subject to boundary conditions 38-40 can be obtained in closed form. It can be shown that the values of the particle displacement u_1 in the two regions is given by

$$u_1(y) = \frac{[\cos\beta - (R/2)^{\frac{1}{2}} \sin\beta\,] - i\,(R/2)^{\frac{1}{2}} \sin\beta}{D} \qquad 0 \leq y \leq \ell \qquad (41)$$

$$u_1(y) = \exp[(i-1)\Gamma(y-\ell)/(\ell\sqrt{2})]/D \qquad y \geq \ell \quad , \qquad (42)$$

where

$$D = \cos\theta - (R/2)^{\frac{1}{2}} \sin\theta - i\,(R/2)^{\frac{1}{2}} \sin\theta, \qquad (43)$$

$$\beta = \theta\,(1-y/\ell) \quad , \qquad (44)$$

$$\theta = \Gamma\sqrt{R} = 2\pi\ell/\lambda_s \quad . \qquad (45)$$

Note that in the limit as $\theta \to 0$ one recovers the solution to the classical Stokes second problem given by

$$u_1(y) = \exp[(i-1)\Gamma(y-\ell)/(\ell\sqrt{2})] \quad . \qquad (46)$$

Two other classical solutions are recoverable from Eqs. (41) and (42). In the case of an inviscid fluid (i.e. $R \to 0$) the solution reduces to

$$u_1(y) = \cos\beta/\cos\theta \quad . \qquad (47)$$

In the case of a very viscous fluid (i.e. $R \to \infty$) the solution reduces to

$$u_1 = \sin\beta/\sin\theta \quad . \qquad (48)$$

Eqs. (47) and (48) correspond to the solutions for shear waves in a finite-thickness elastic medium with a free and a fixed boundary. Conditions for $\theta = (1+2n)\pi/2$ and $\theta = 2n\pi$ for the former and the latter case correspond to the resonance conditions associated with a closed-open and a closed-closed pipe respectively [5].

The solution to the MSSP as represented by Eqs. (41) and (42) together with the limiting cases (47) and (48) will become very useful in understanding the results obtained in the presence of a transition layer.

III - DISCUSSION OF RESULTS

III-1 Displacement-Driven Boundary

In the discussion that follows, the results are presented in the form of particle displacement and shear stress distribution as function of distance from the lower boundary; a unit wall disturbance is applied at the lower boundary of the coating. The numerical integration of the equation of motion for the conditions of very thin transition layer (i.e. $n \to \infty$) should give results which agree with the solution to the MSSP discussed in the previous section. Figures 6 and 7 show the particle and the shear stress distribution for typical conditions of four increasingly thinner transition layers. The numerical solutions are seen to asymptote to the proper limiting solution. The transition layer for the four values of n considered (n = 8, 16, 32, 64) correspond to thicknesses of about 0.5ℓ , 0.25ℓ , 0.12ℓ and 0.06ℓ respectively. It is interesting to note that as the transition layer thickness increases, a particle displacement overshoot (i.e. local displacement larger than unity) begins to appear. The overshoot becomes more evident as either Γ or R is increased. Physically these conditions correspond to higher frequency, thicker elastic layer and softer coating material (lower C_s). Figs. 8 and 9 show the effect of thicker elastic layers (bigger Γ) while Figs. 10 and 11 show the effect of softer coating materials (higher R). In both instances the transition layer thickness has been fixed to correspond to n = 8. Reducing the transition layer thickness will cut down on the magnitude of the overshoot but will be eliminated only in the limit as $n \to \infty$. A transition layer equal to 0.5ℓ (n=8) will produce a 48% overshoot while a 0.25ℓ thick layer will produce a 20% overshoot. These values are for $R = 10^{-5}$ and $\Gamma = 50$ (Fig. 12). The no-transition layer results agree exactly with the present analysis at all locations except for values of y in the neighborhood of the overshoot. The overshoot produced by the classical approach (i.e. no transition layer) is minimal and it cannot be seen on the scales used in the figures. The relative magnitude of the overshoot is a function of the transition layer thickness and elastic layer properties.

The physical reasoning for the overshoot can be best understood by referring to the analytical solution of the MSSP (Eqs. 41 and 42). Evaluating the particle displacement at the solid-fluid interface gives

$$u_1(\ell) = D^{-1} \quad . \tag{49}$$

Values of Γ and R which will minimize D will maximize the particle displacement at the interface and in its neighborhood. It is instructive to note that in the limiting condition of an inviscid fluid (i.e. R→0) and with $\Theta = \pi/2$ (i.e. coating thickness ℓ equal to one quarter of shear wavelength of solid) one will obtain very large particle displacements at the interface. This result is consistent with the concept of a velocity (or displacement) driven open pipe having waves reflected at the open end of the pipe and creating resonance conditions. The displacement overshoots are thus seen to be caused by the reflection of the shear waves at the solid-fluid interface. The presence of a viscoelastic non-homogeneous transition layer at the interface is seen to magnify the internal reflection of the waves. The actual magnitude of the magnification is a function of the three parameters Γ, R and n.

III-2 Force-Driven

For conditions where the lower boundary of the elastic layer is force-driven, the wall boundary conditions applicable to the numerical integration of Eq. 25 is

$$\left.\frac{du_1}{dy}\right|_{y=0} = 1 \quad . \tag{31-a}$$

The value of the wall displacement $u_1(0)$ is iterated until the proper far-field radiation condition is obtained.

Two typical cases of force-driven conditions are shown in Figs. 13-15. When the displacement profiles are non-dimensionalized with respect to the wall displacements, the results collapse on the same curve obtained for the displacement-driven condition (see Fig. 16). The same conclusion applies to the shear stress distribution. It should also be noted that, as expected, the Rayleigh reciprocal theorem ($\tau_1 U_2 = \tau_2 u_1$) holds. This result can be verified by noting that at any y location the product of the stress from the dislacement-driven case multiplied by the displacement from the force-driven condition equals the product of the stress from the force-driven case with the displacement from the displacement-driven condition.

IV - CONCLUSIONS

The effect of a viscoelastic non-homogeneous transition layer located at the interface between an elastic solid and a viscous fluid has been analyzed. The displacement and the stress distribution due to either a displacement or a stress-driven lower boundary have been analyzed. It has been shown that a thin layer can radically change the reflection characteristics of the interface in such manner as to magnify the displacement overshoot that is normally present.

Results have been presented and discussed for displacement and for force-driven coating disturbances. No basic differences exist between the two solutions. The present results have been analyzed with and compared to the analytic solution of the modified Stokes second problem.

REFERENCES

1. An Introduction to Fluid Dynamics, G. K. Batchelor, Cambridge University Press, 197.

2. R. P. Johnson, "Review of Compliant Coating Research of M. O. Kramer, 1957-1975," RPJ Associates, Sept. 1980.

3. Foundations of Solid Mechanics, Y. C. Fung, Prentice-Hall Inc., 1965.

4. Boundary Layer Theory, H. Schlichting, McGraw-Hill, 1960.

5. Fundamentals of Acoustics, L. E. Kinsler and A. R. Frey, Wiley & Sons, 1962.

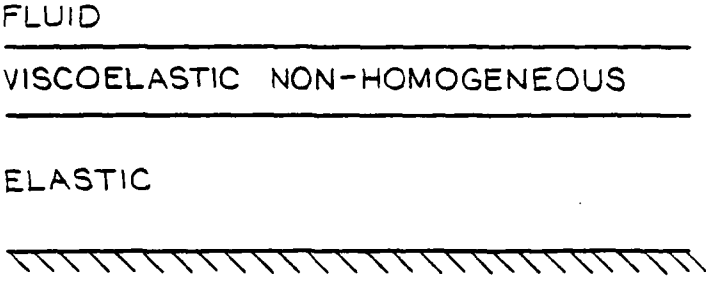

(a)

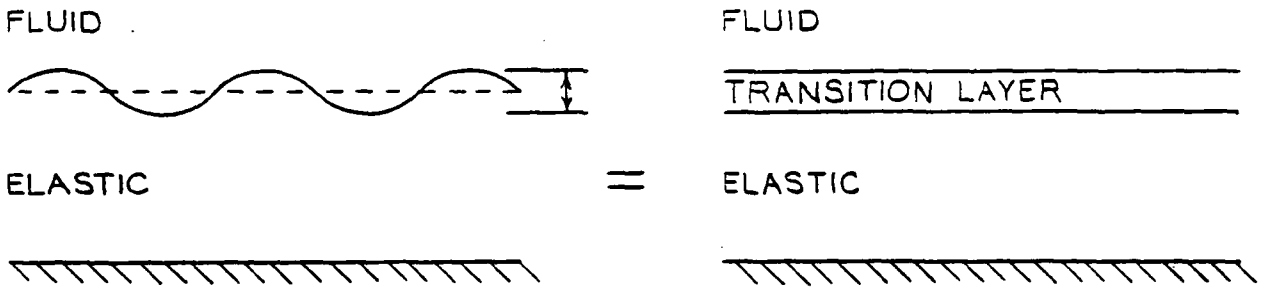

(b)

FIG. 1 – TRANSITION LAYER MODELS – (a) VISCOELASTIC NON-HOMOGENEOUS LAYER – (b) EQUIVALENT TRANSITION LAYER DUE TO SURFACE MOTION.

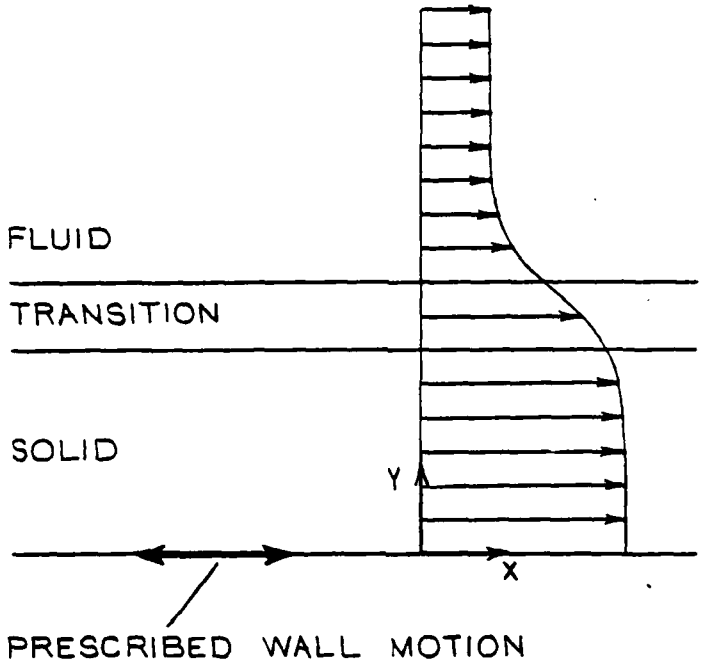

FIG. 2 – ONE-DIMENSIONAL TRANSVERSE WAVES IN SOLID, TRANSITION LAYER, AND FLUID.

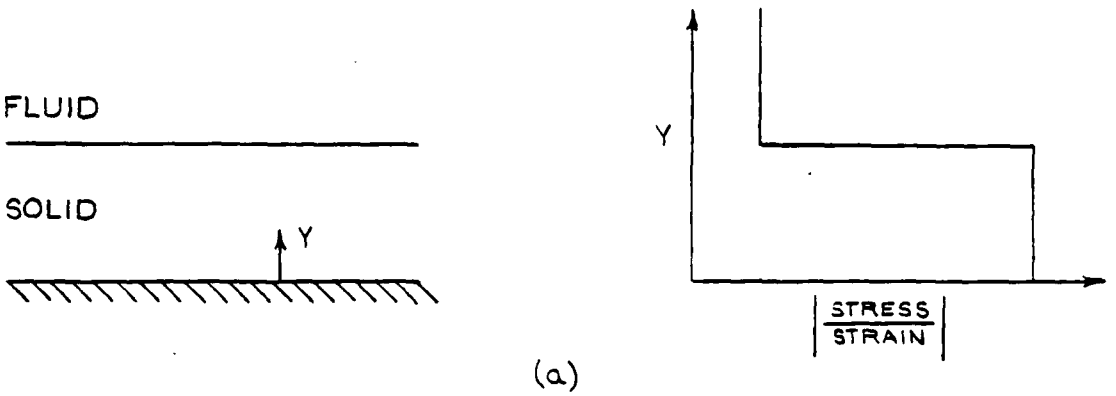

(a)

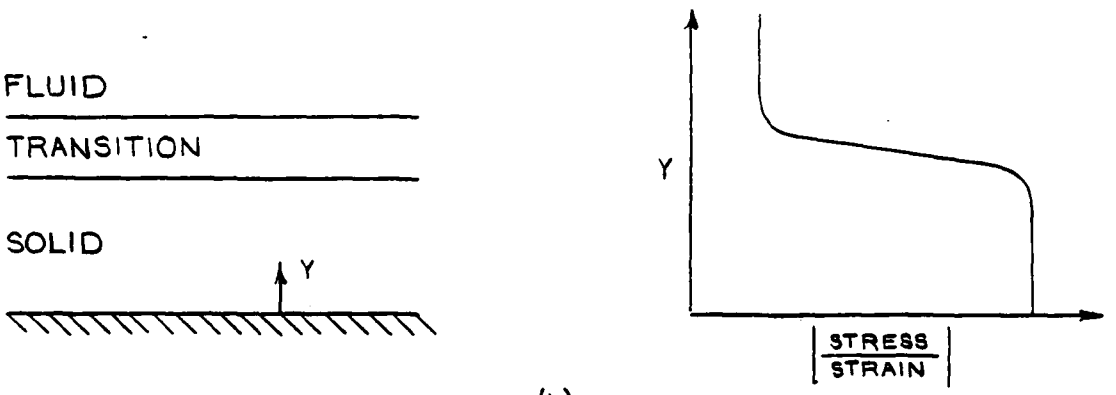

(b)

FIG. 3 – VARIATION OF THE STRESS-STRAIN COEFFICIENT AS A FUNCTION OF WALL DISTANCE FOR (a) NO TRANSITION, (b) WITH TRANSITION LAYER.

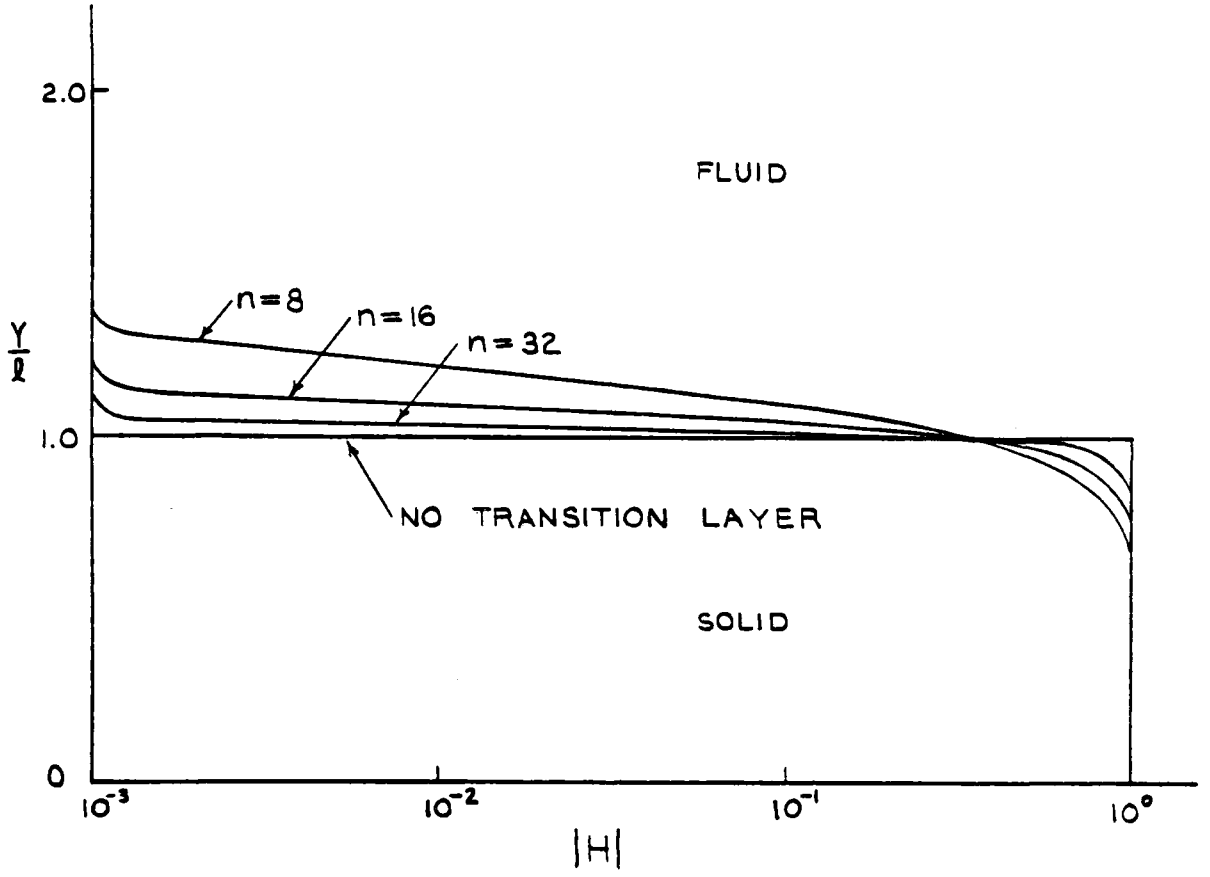

FIG. 4 - TRANSITION LAYER CHARACTERISTICS. $R=10^{-3}$.

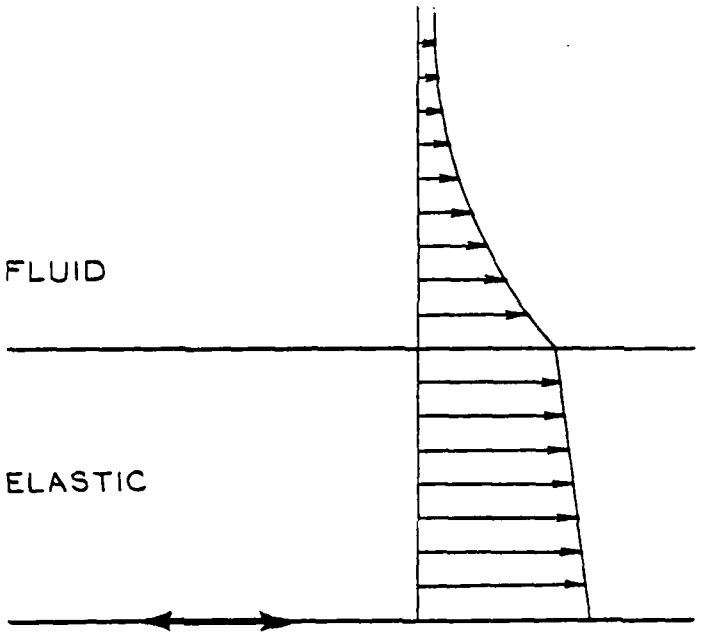

FIG. 5 – MODIFIED STOKES SECOND PROBLEM - MSSP.

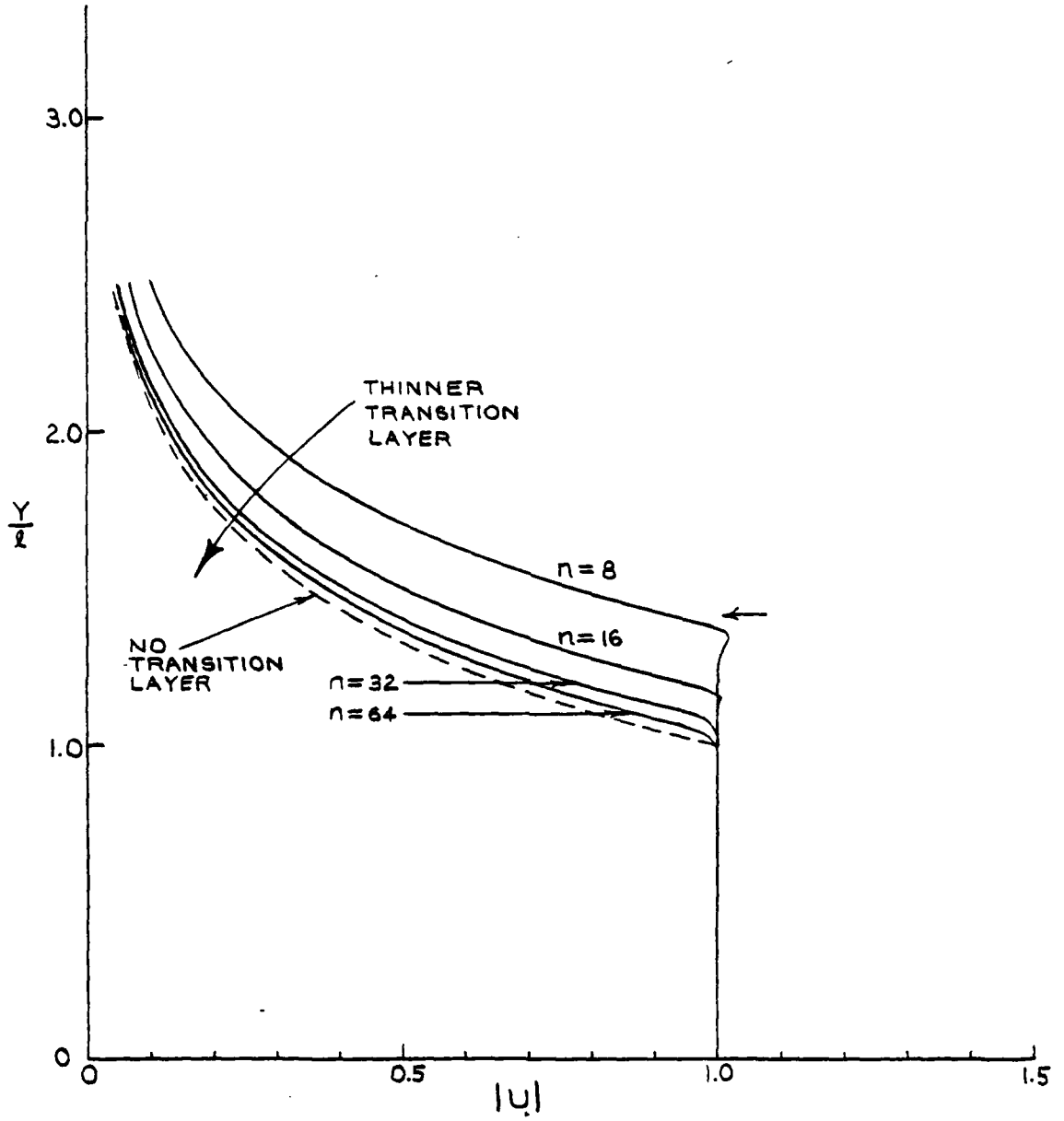

FIG. 6 – PARTICLE DISPLACEMENT DISTRIBUTION – EFFECT OF TRANSITION LAYER THICKNESS. $R=10^{-5}$, $\Gamma=3$

← OUTER EDGE OF TRANSITION LAYER.

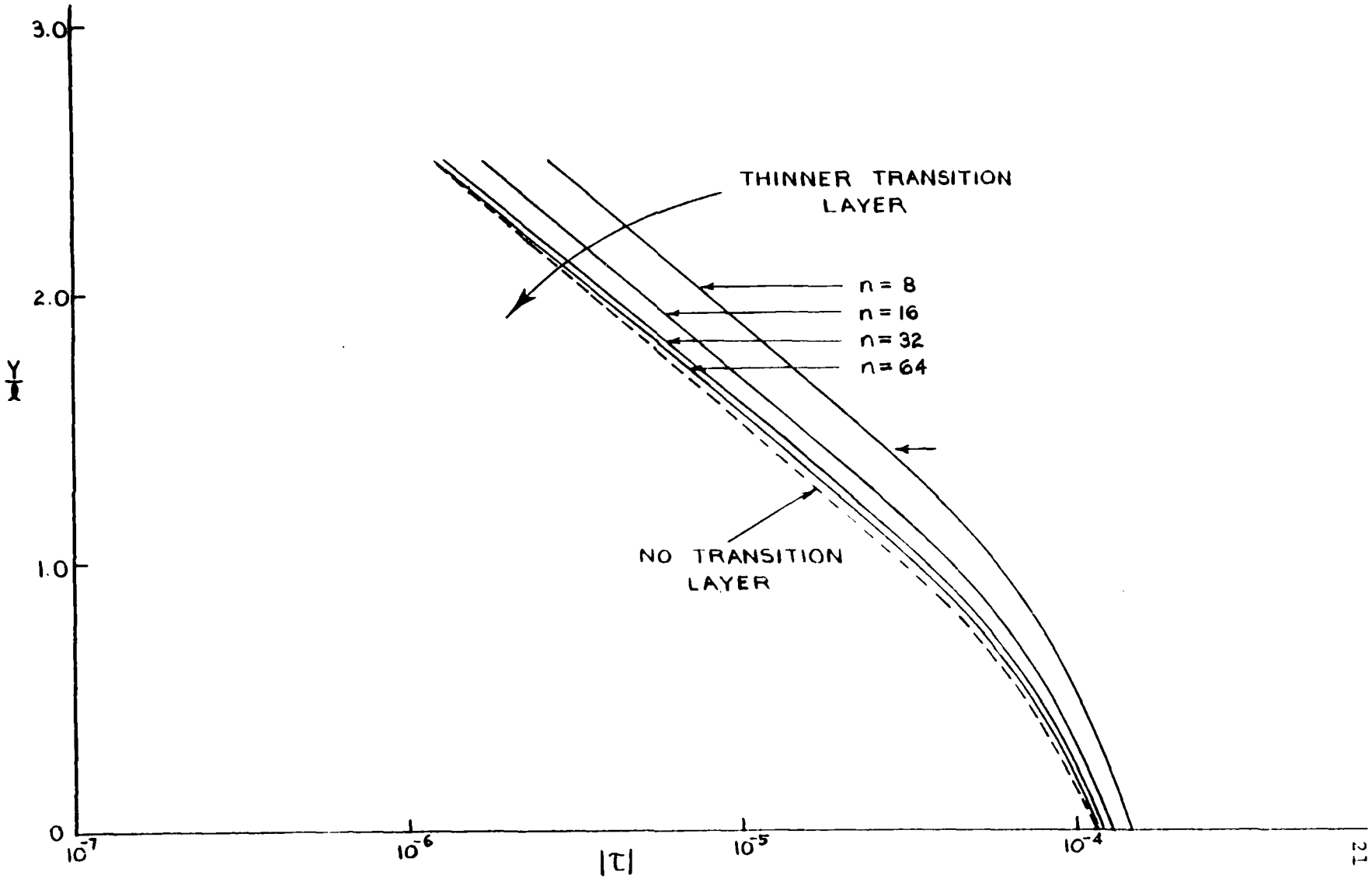

FIG.7 - SHEAR STRESS DISTRIBUTION AS FUNCTION OF TRANSITION LAYER THICKNESS. $R=10^{-5}$, $\Gamma=3$.

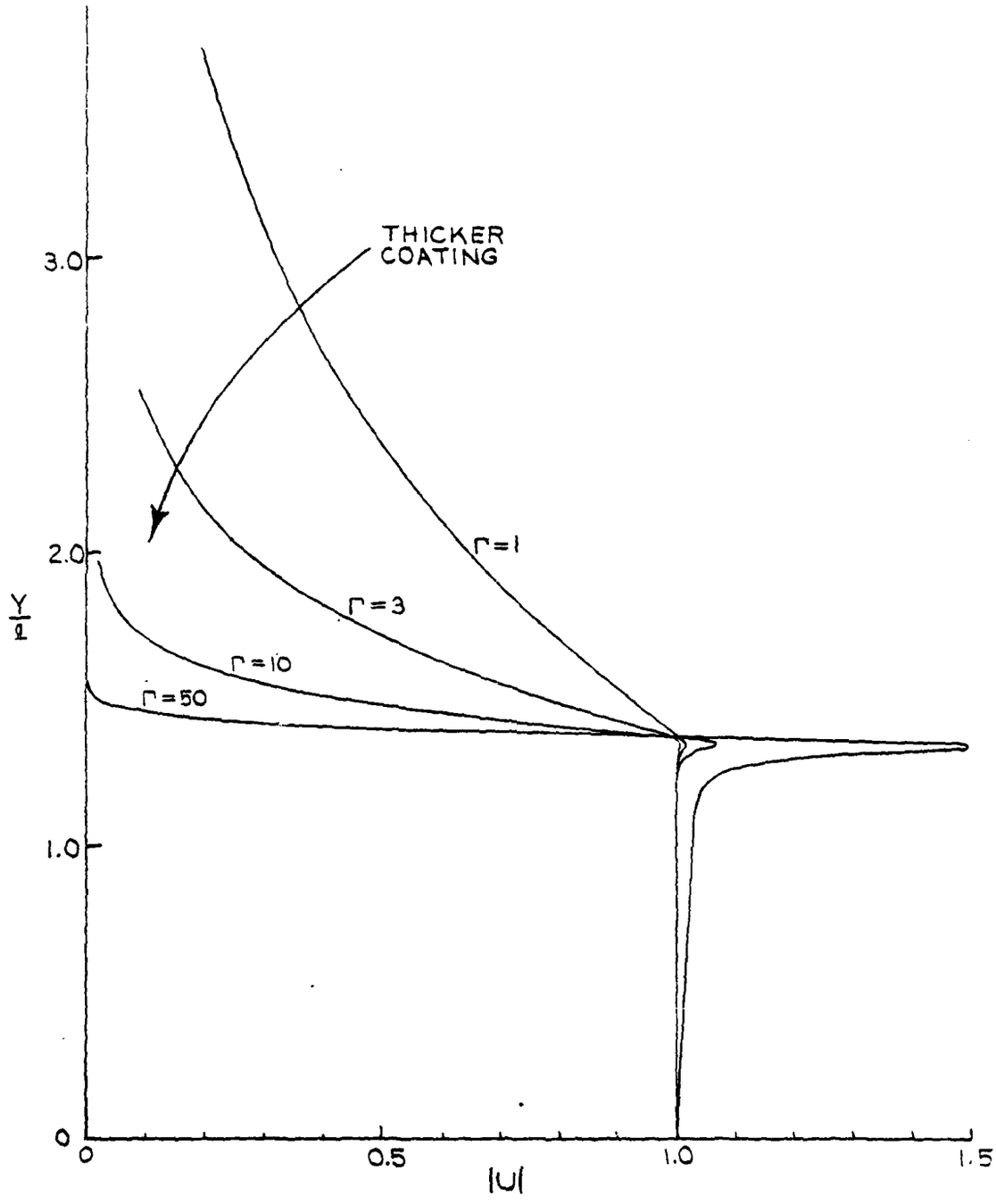

FIG.8-PARTICLE DISPLACEMENT DISTRIBUTION FOR DIFFERENT COATING THICKNESSES. $R=10^{-5}$, $n=8$.

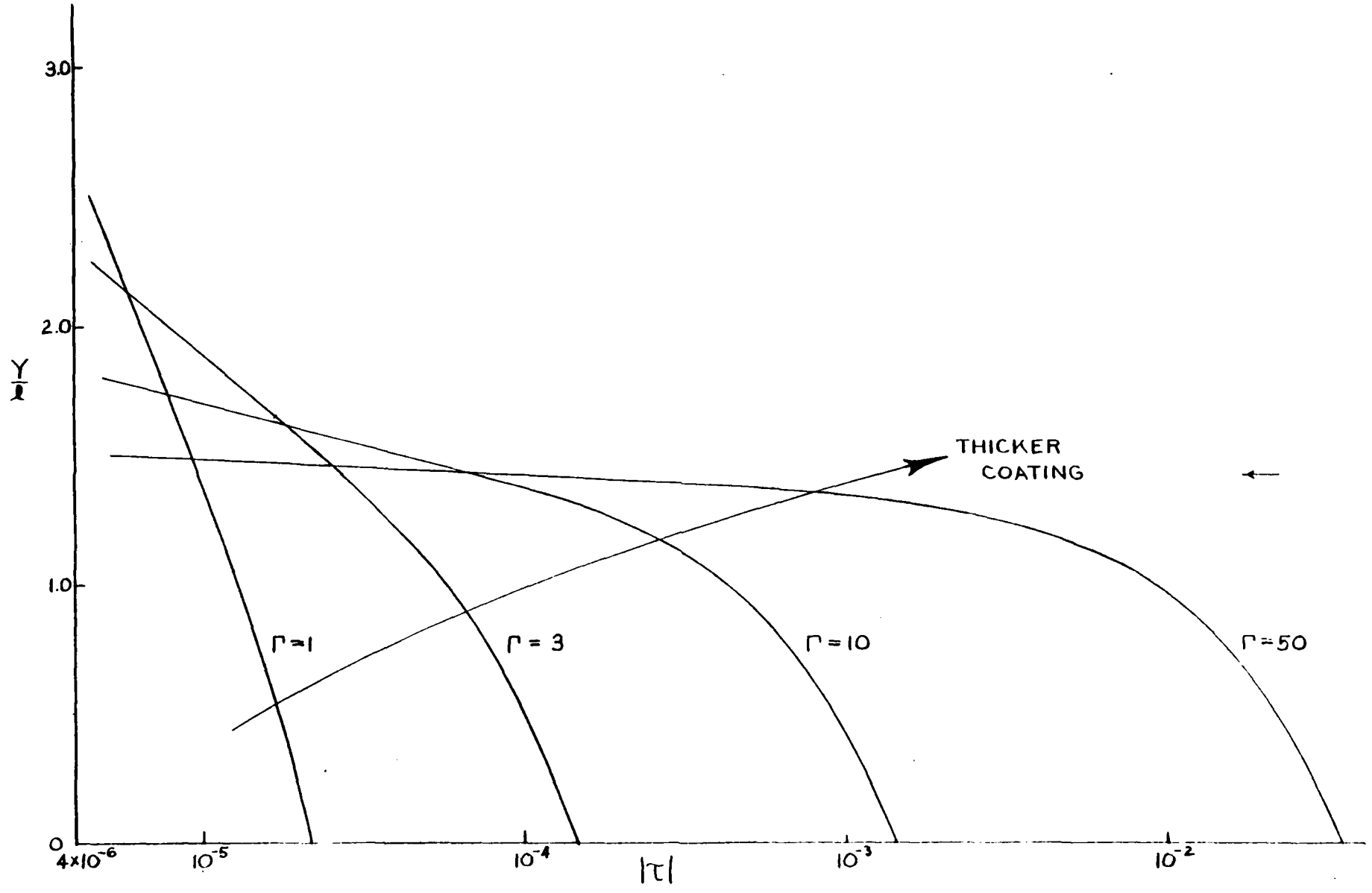

FIG.9-SHEAR STRESS DISTRIBUTION AS FUNCTION OF COATING THICKNESS.
$n=8$ $R=10^{-5}$.

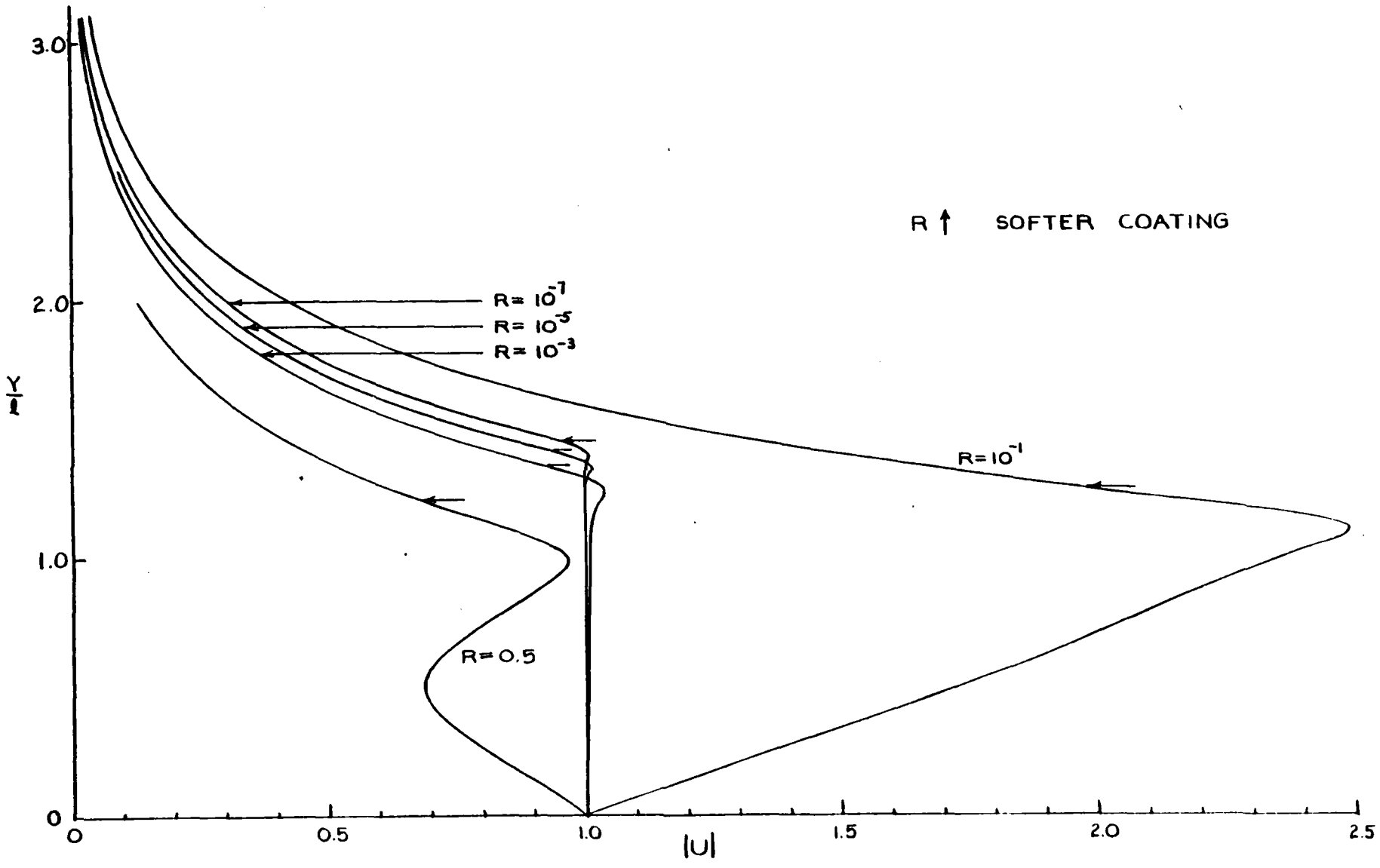

FIG. 10-PARTICLE DISPLACEMENT DISTRIBUTION – EFFECT OF COATING PROPERTIES. $n=8, \Gamma=3$.

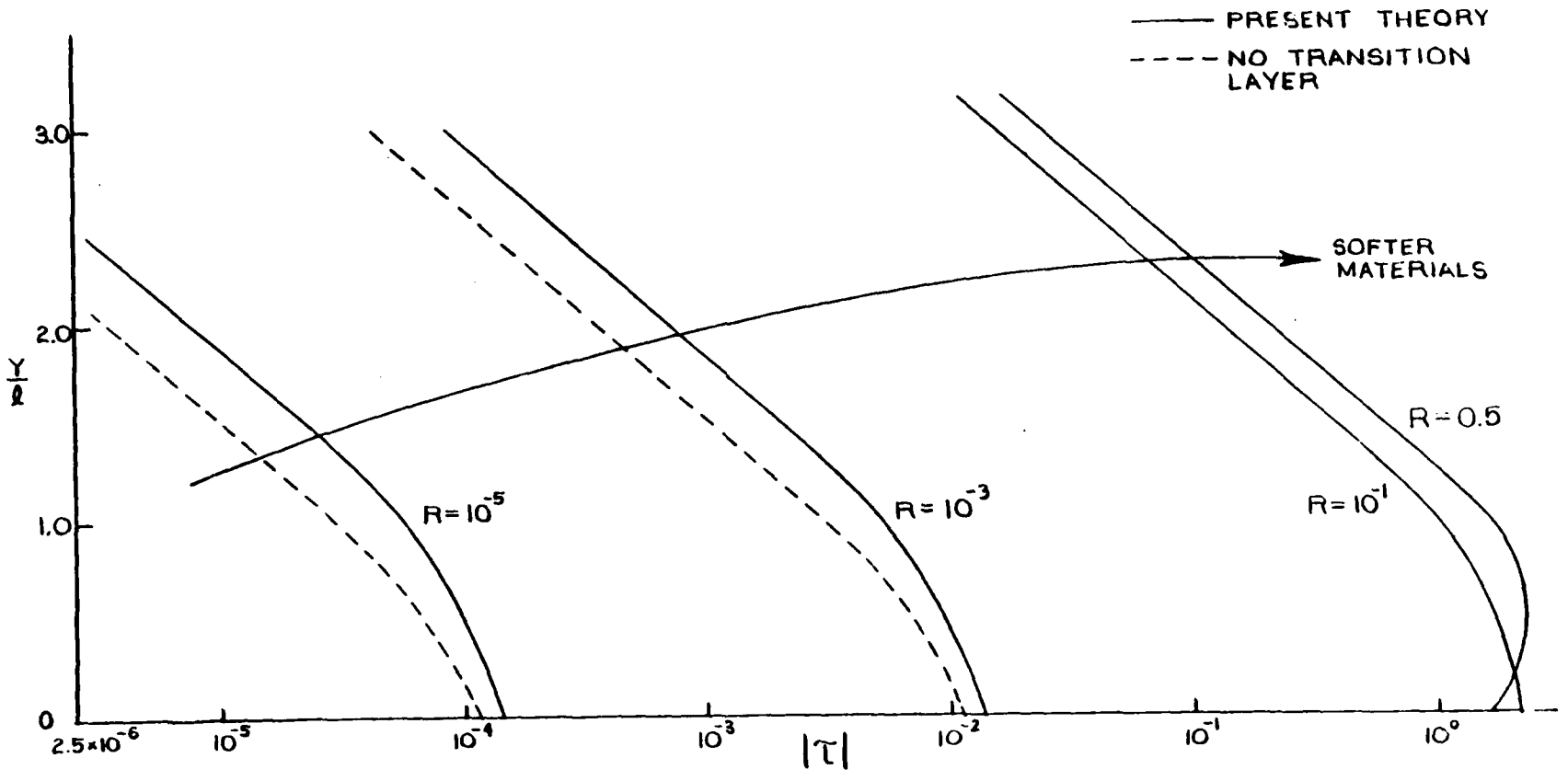

FIG.11 - SHEAR STRESS DISTRIBUTION AS FUNCTION OF COATING MATERIALS.
$n = 8, \Gamma = 3$.

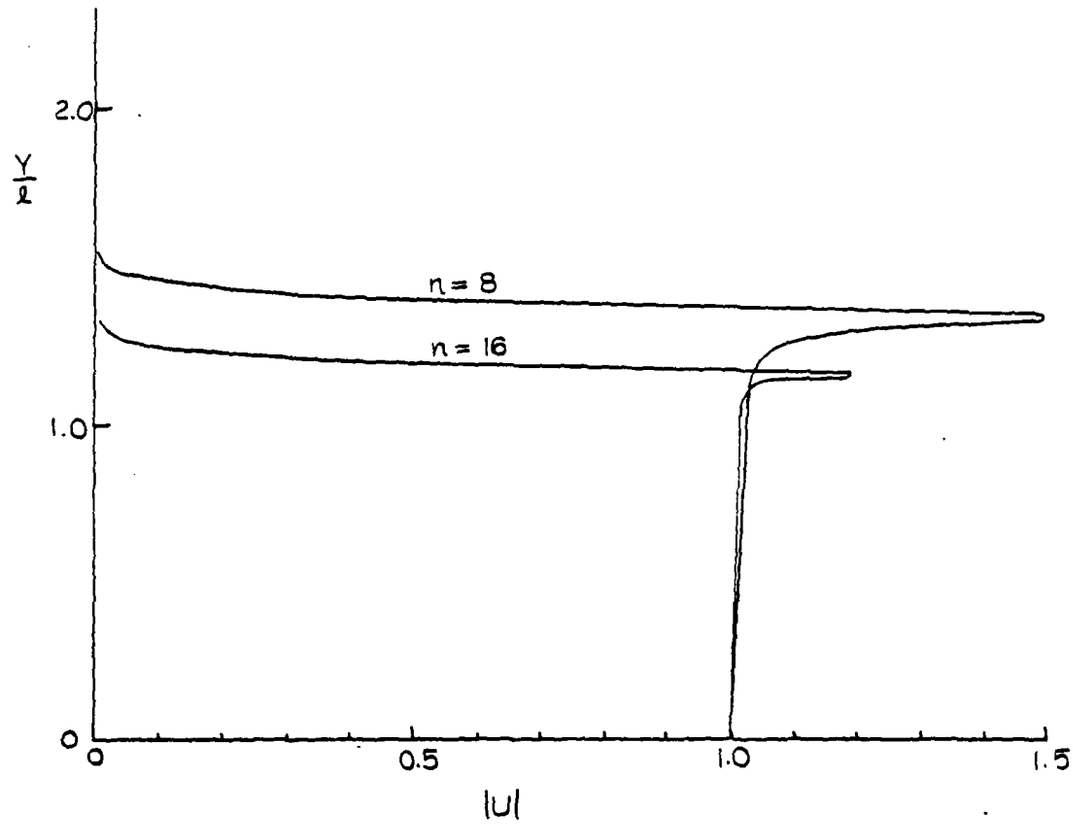

FIG. 12 – EFFECT OF TRANSITION LAYER THICKNESS ON DISPLACEMENT DISTRIBUTION. $R=10^{-5}$, $\Gamma=50$.

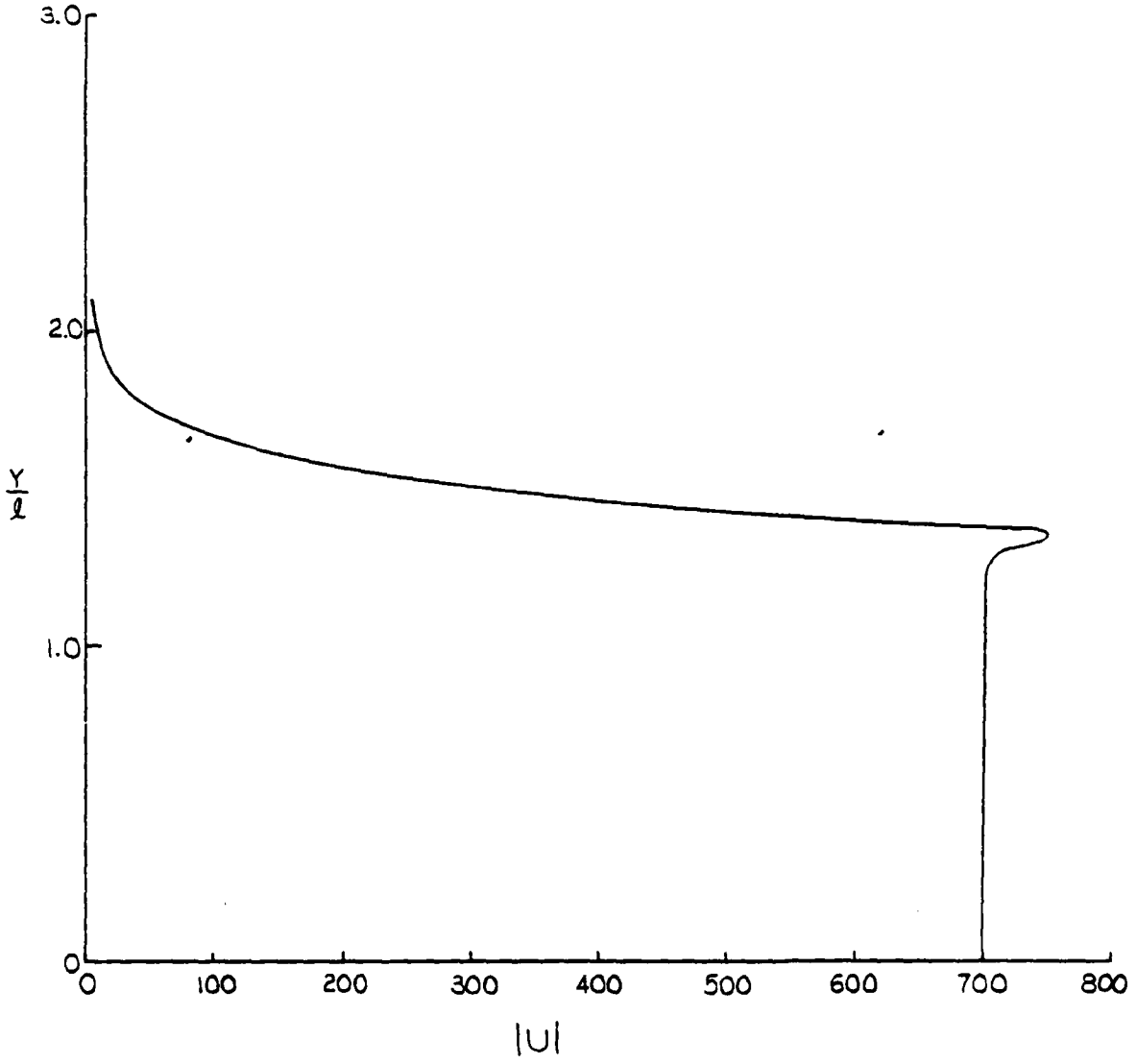

FIG. 13 – PARTICLE DISPLACEMENT DISTRIBUTION FOR FORCE-DRIVEN BOUNDARY. $n=8, R=10^{-5}, \Gamma=10$.

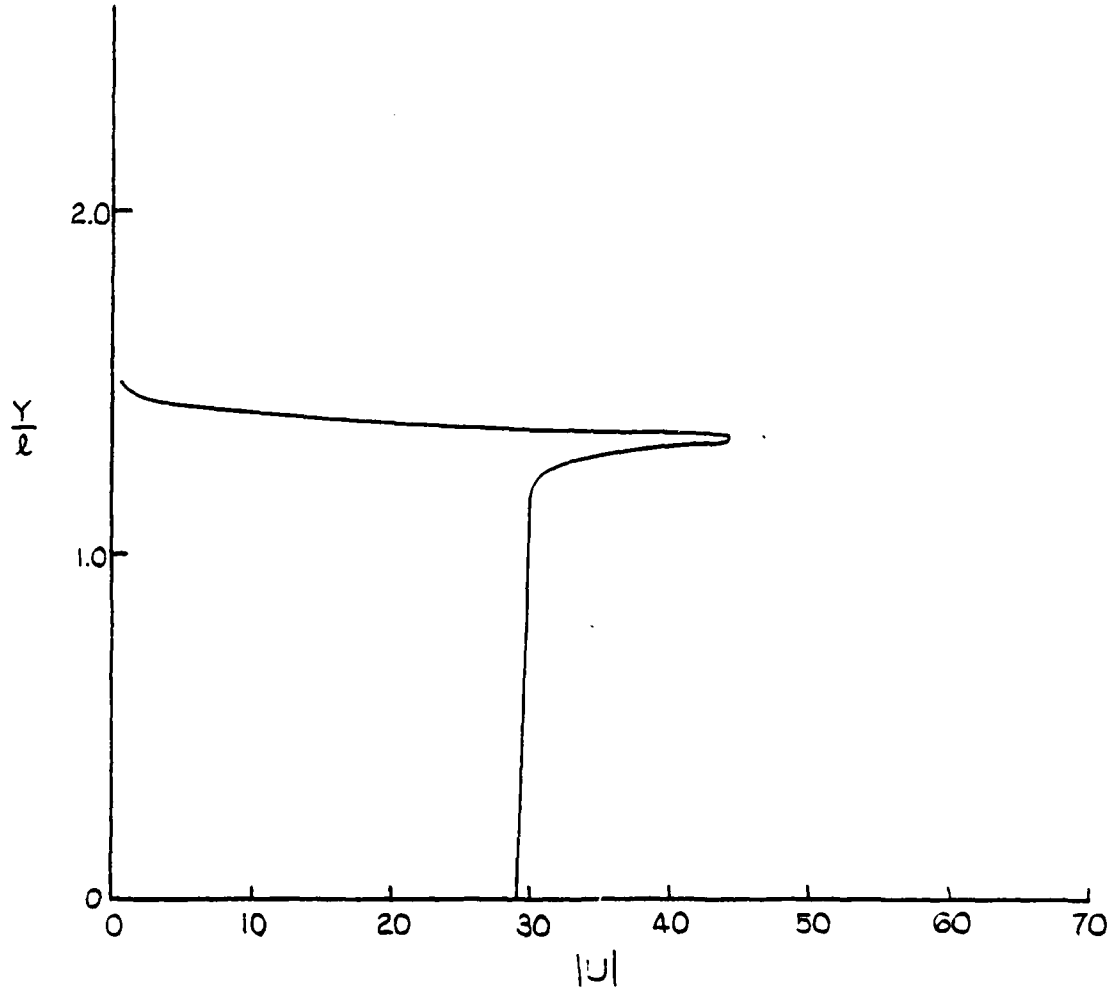

FIG. 14 - PARTICLE DISPLACEMENT DISTRIBUTION FOR FORCE-DRIVEN BOUNDARY. $n=8$, $R=10^{-5}$, $\Gamma=50$.

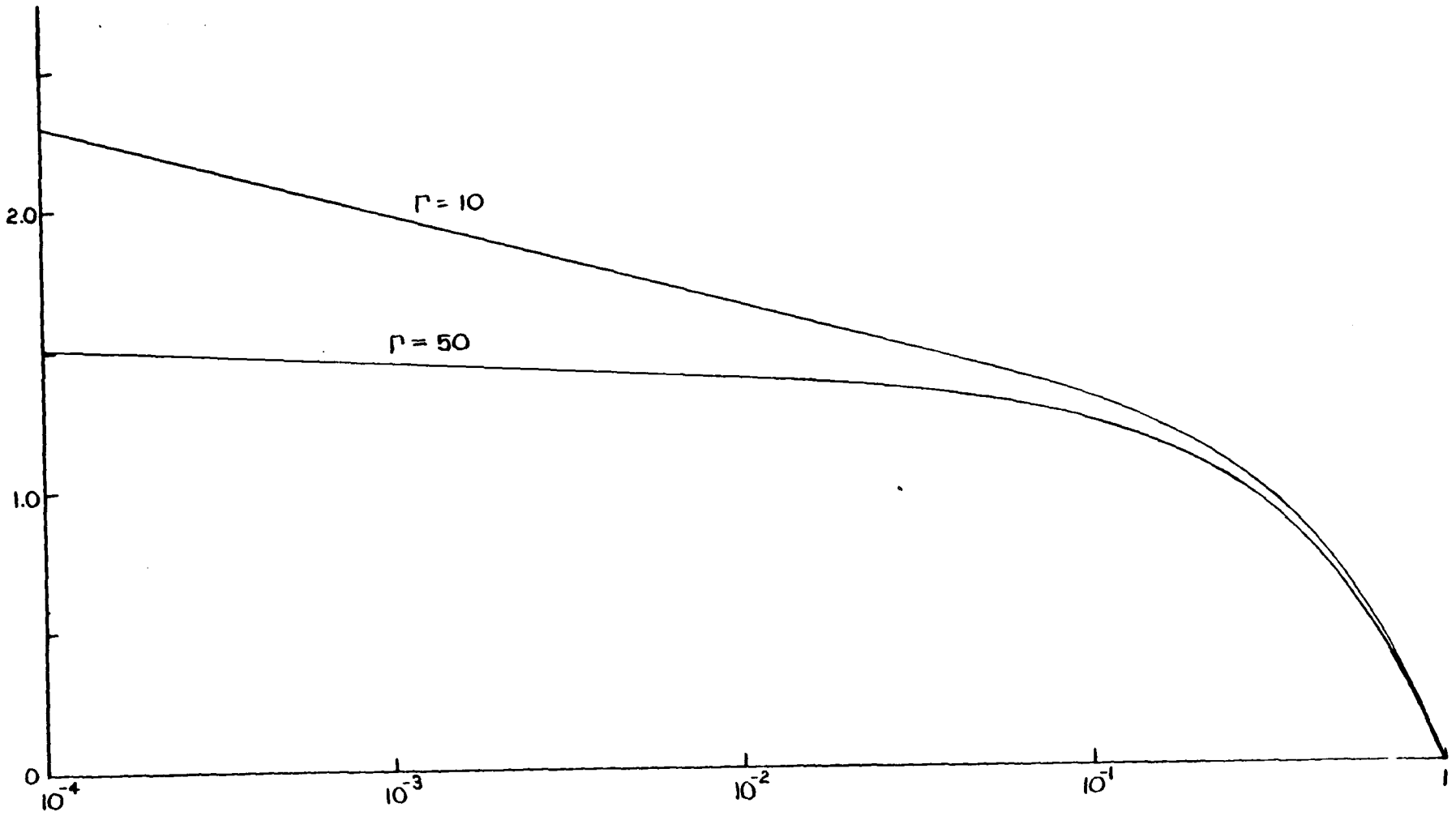

FIG. 15 – SHEAR STRESS DISTRIBUTION FOR FORCE-DRIVEN BOUNDARY. n=8, $R = 10^{-5}$.

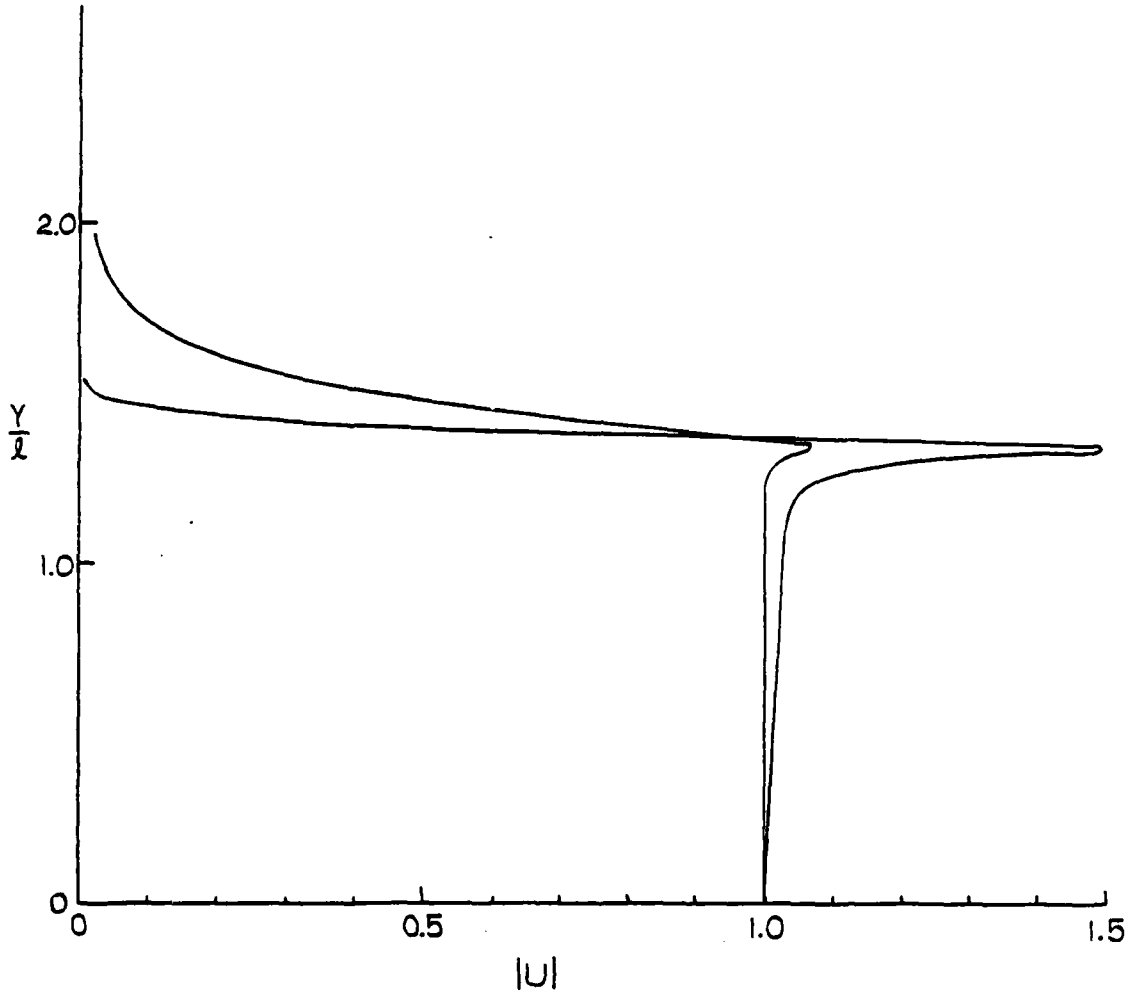

FIG. 16 – NORMALIZED PARTICLE DISPLACEMENT DISTRIBUTION FOR FORCE-DRIVEN BOUNDARY. $n=8$, $R=10^{-5}$.

APPENDIX

Enclosed are additional figures of particle displacement and shear stress distribution.

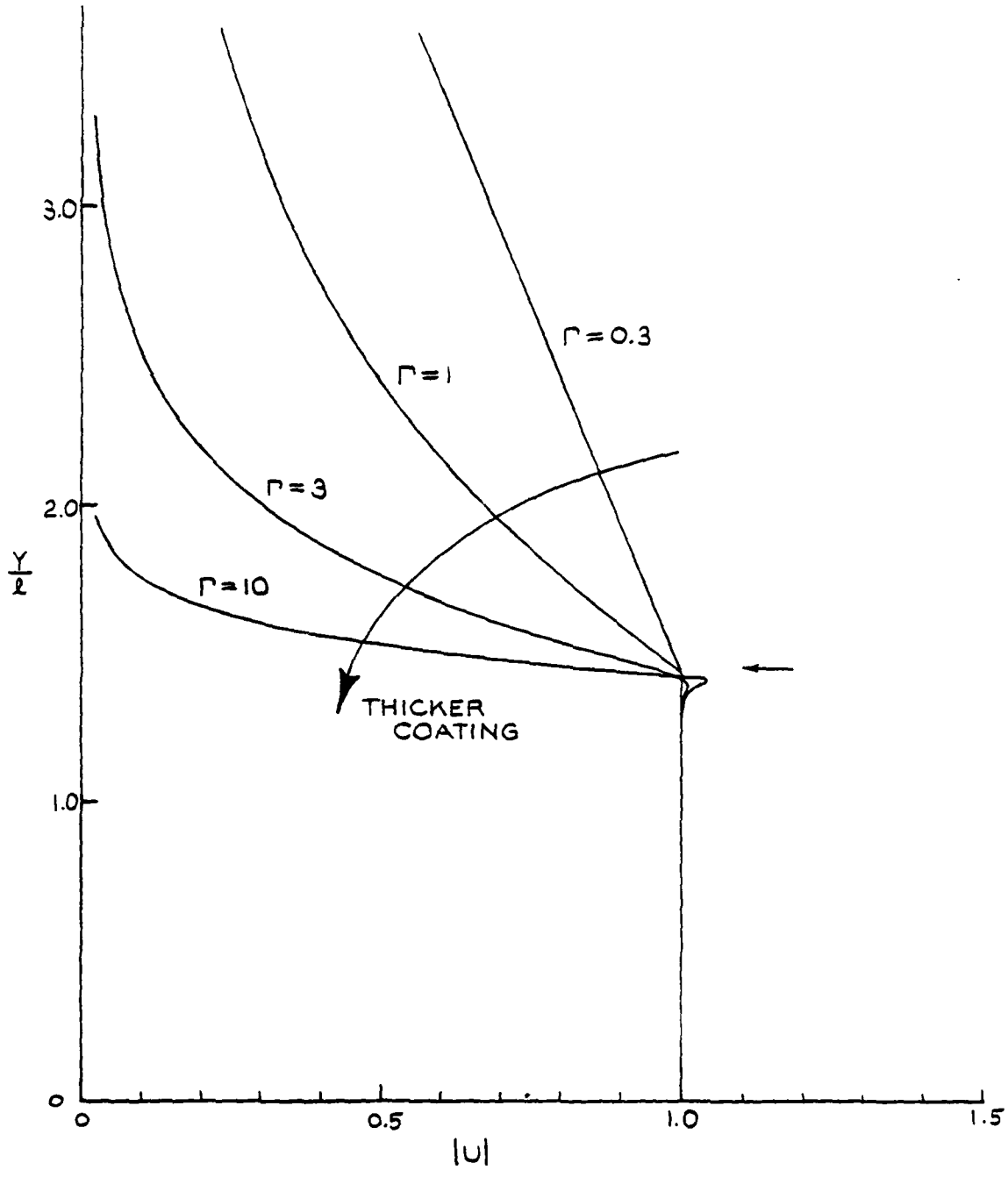

FIG. A-1 – PARTICLE DISPLACEMENT DISTRIBUTION FOR DIFFERENT COATING THICKNESSES. $n=8$, $R=10^{-7}$.

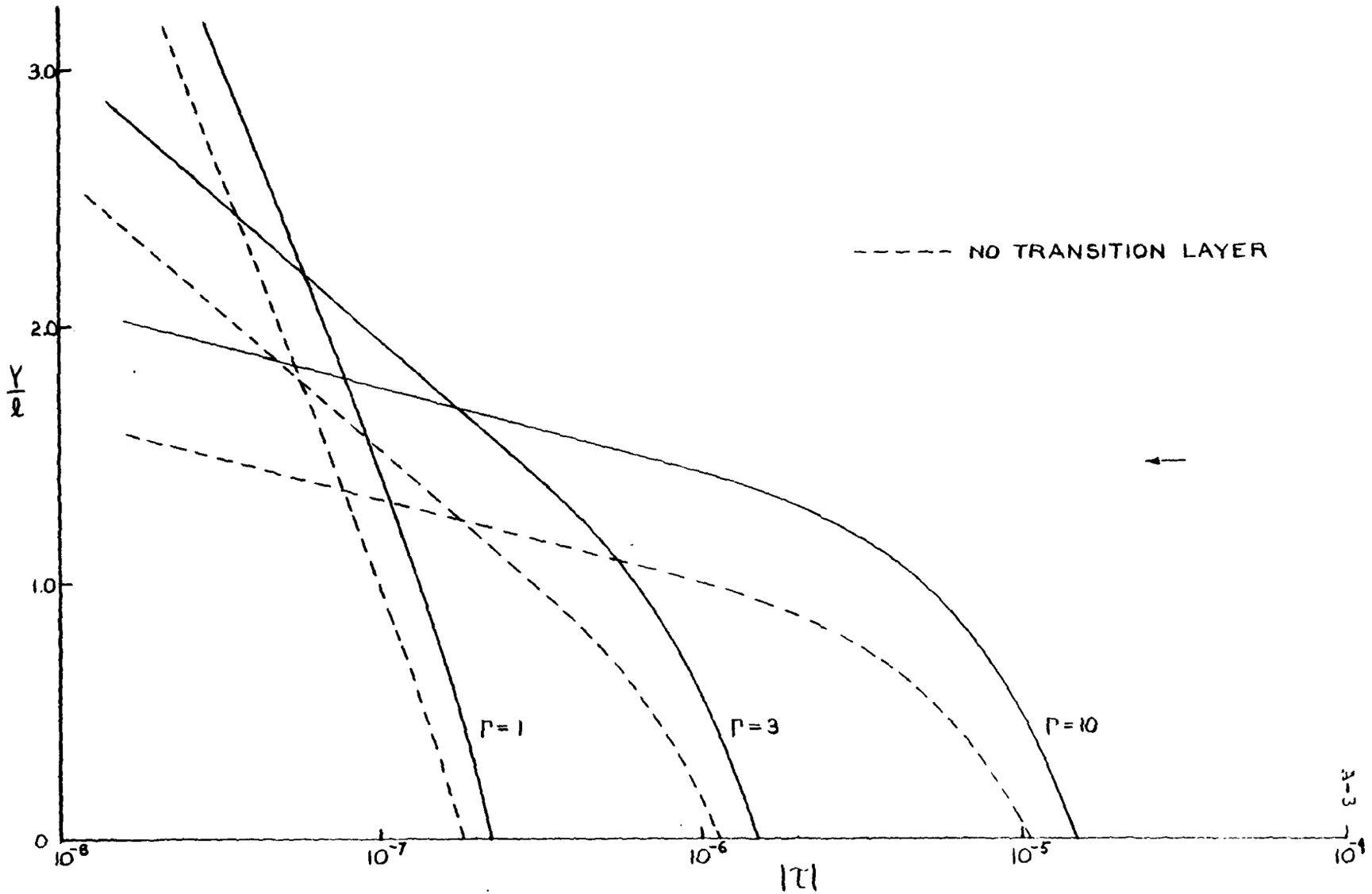

FIG. A-2 – SHEAR STRESS DISTRIBUTION AS FUNCTION OF COATING THICKNESS. $n=8$, $R=10^{-7}$.

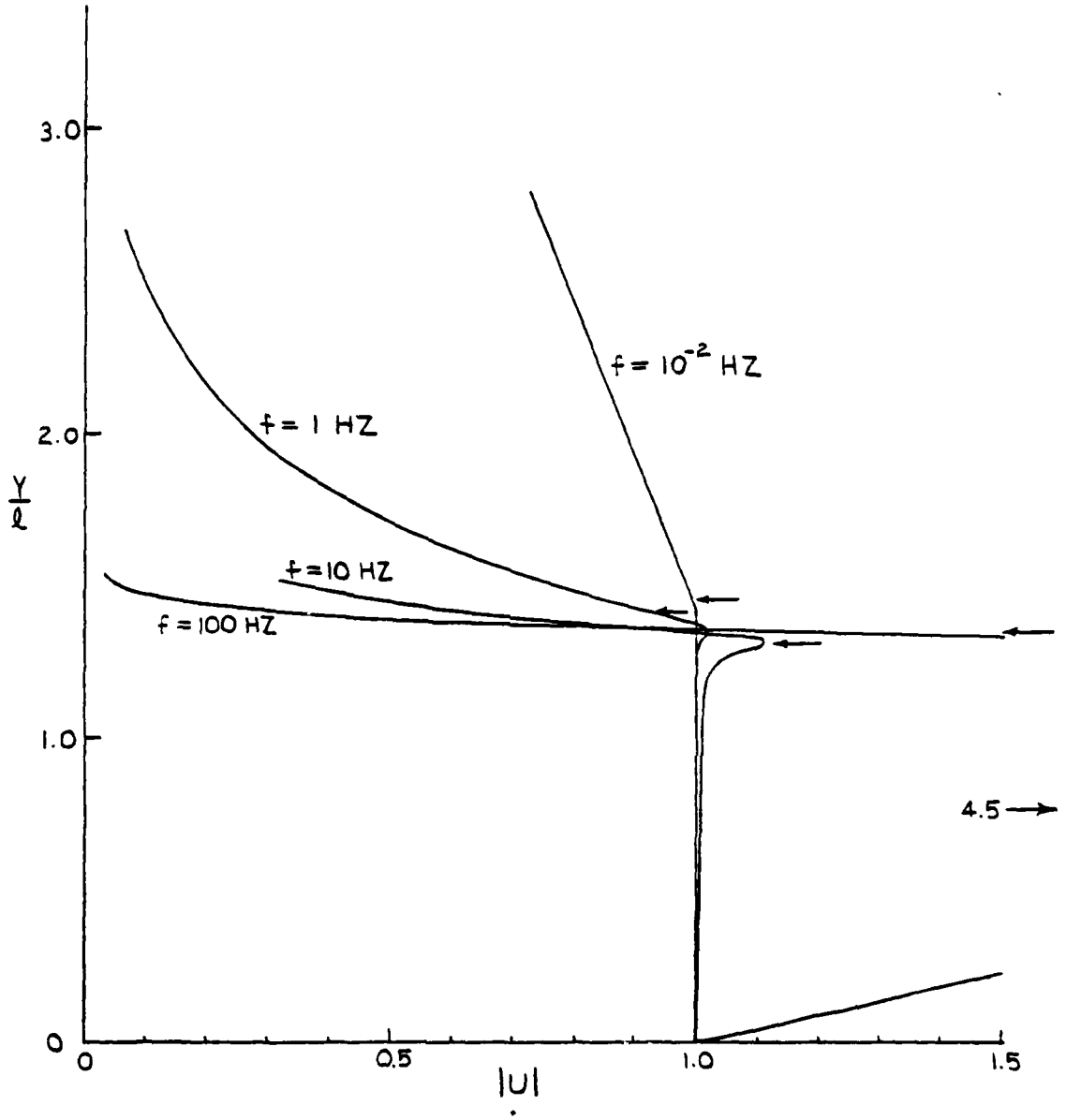

FIG. A-3 – PARTICLE DISPLACEMENT DISTRIBUTION AS FUNCTION OF FREQUENCY FOR TYPICAL COMPLIANT COATING. $n=8$, $\ell = 1.25$ mm, $c_s = 0.8$ m/sec

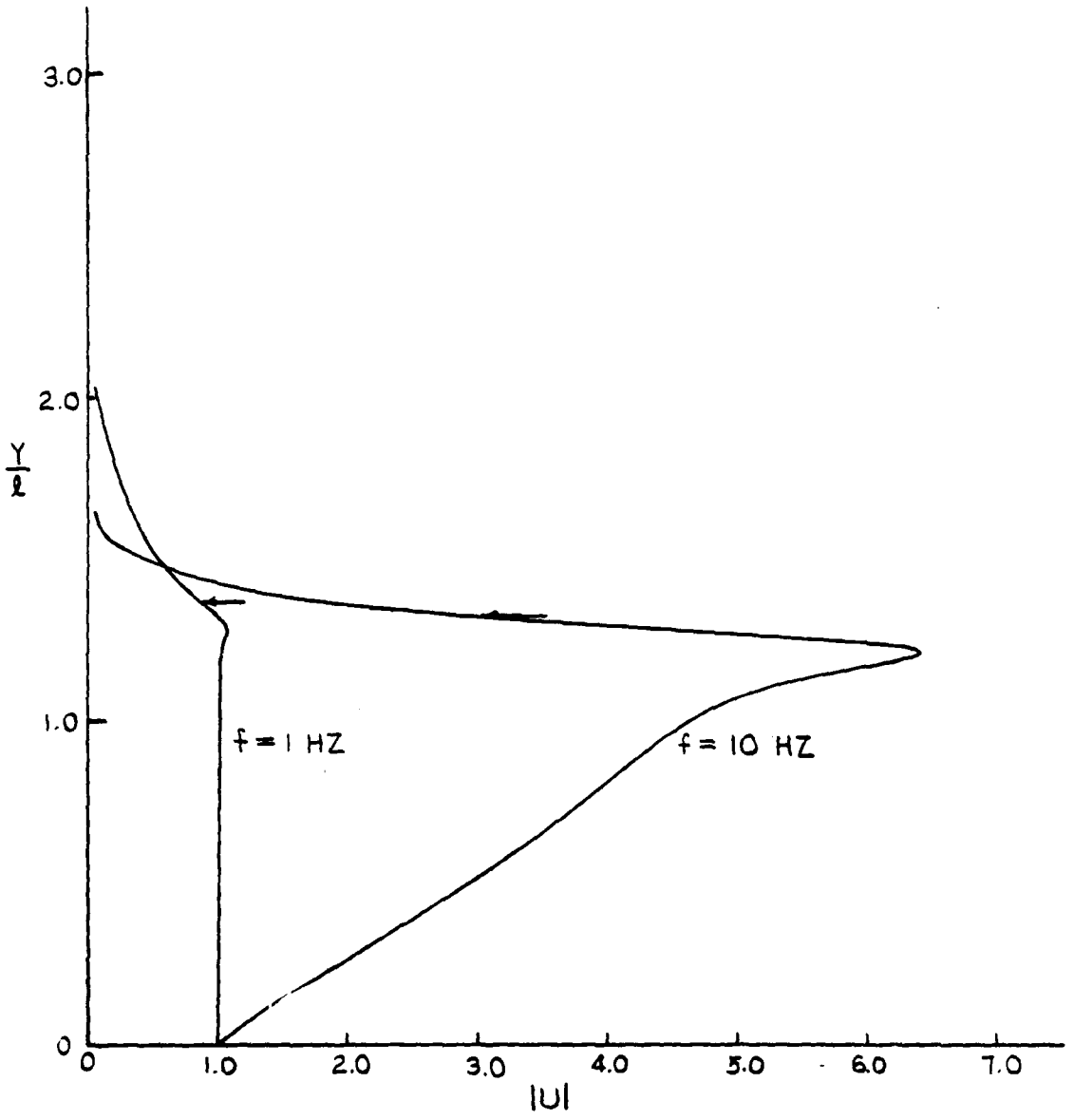

FIG. A-4 - PARTICLE DISPLACEMENT DISTRIBUTION AS FUNCTION OF FREQUENCY FOR TYPICAL COMPLIANT COATING. $n=8$, $\ell=2.5\,mm$, $C_s=0.1$ m/sec.

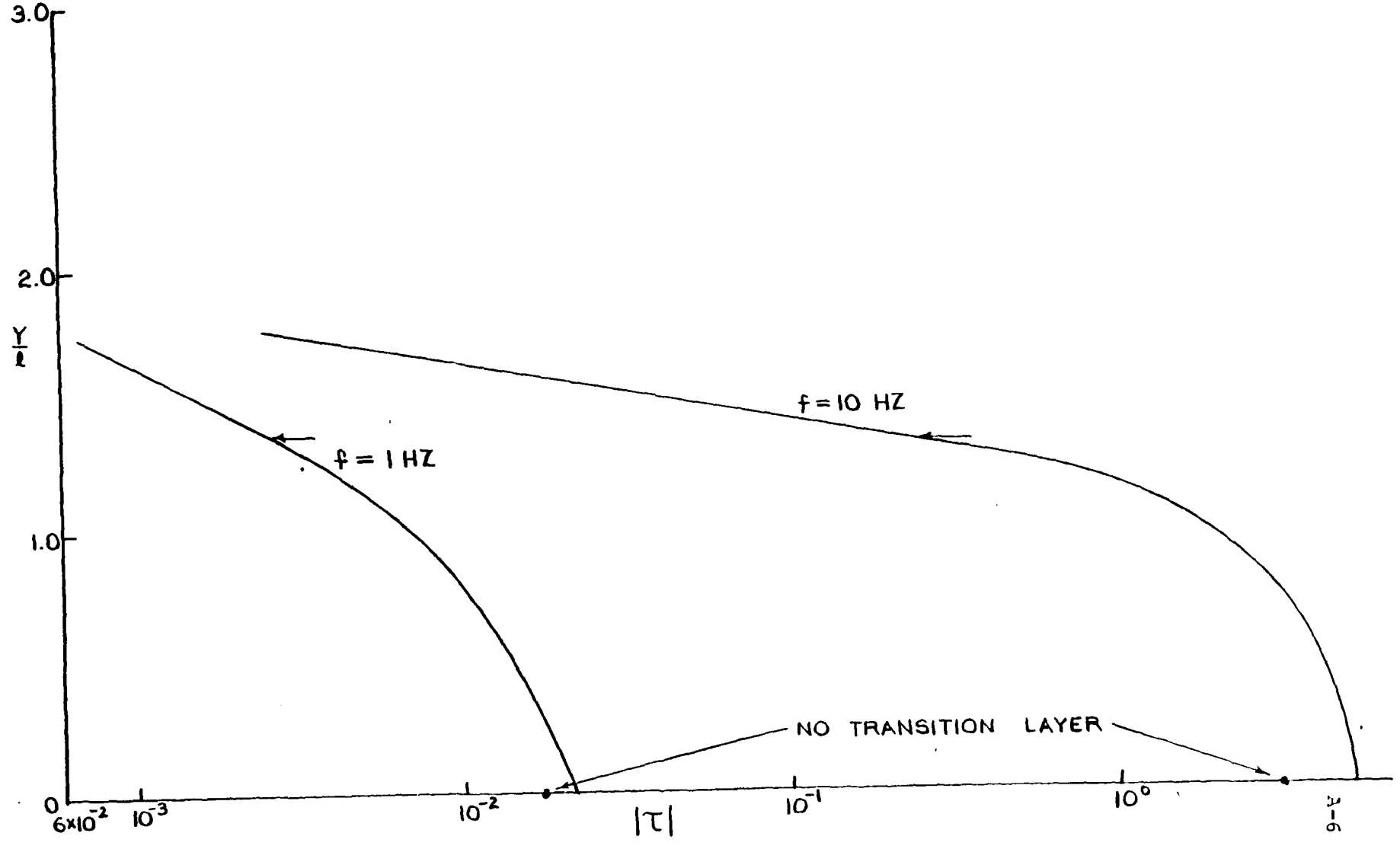

FIG. A-5 - SHEAR STRESS DISTRIBUTION AS FUNCTION OF FREQUENCY FOR TYPICAL COMPLIANT COATING. $n = 8$, $\ell = 2.5$ mm, $C_s = 0.1$ m/sec.

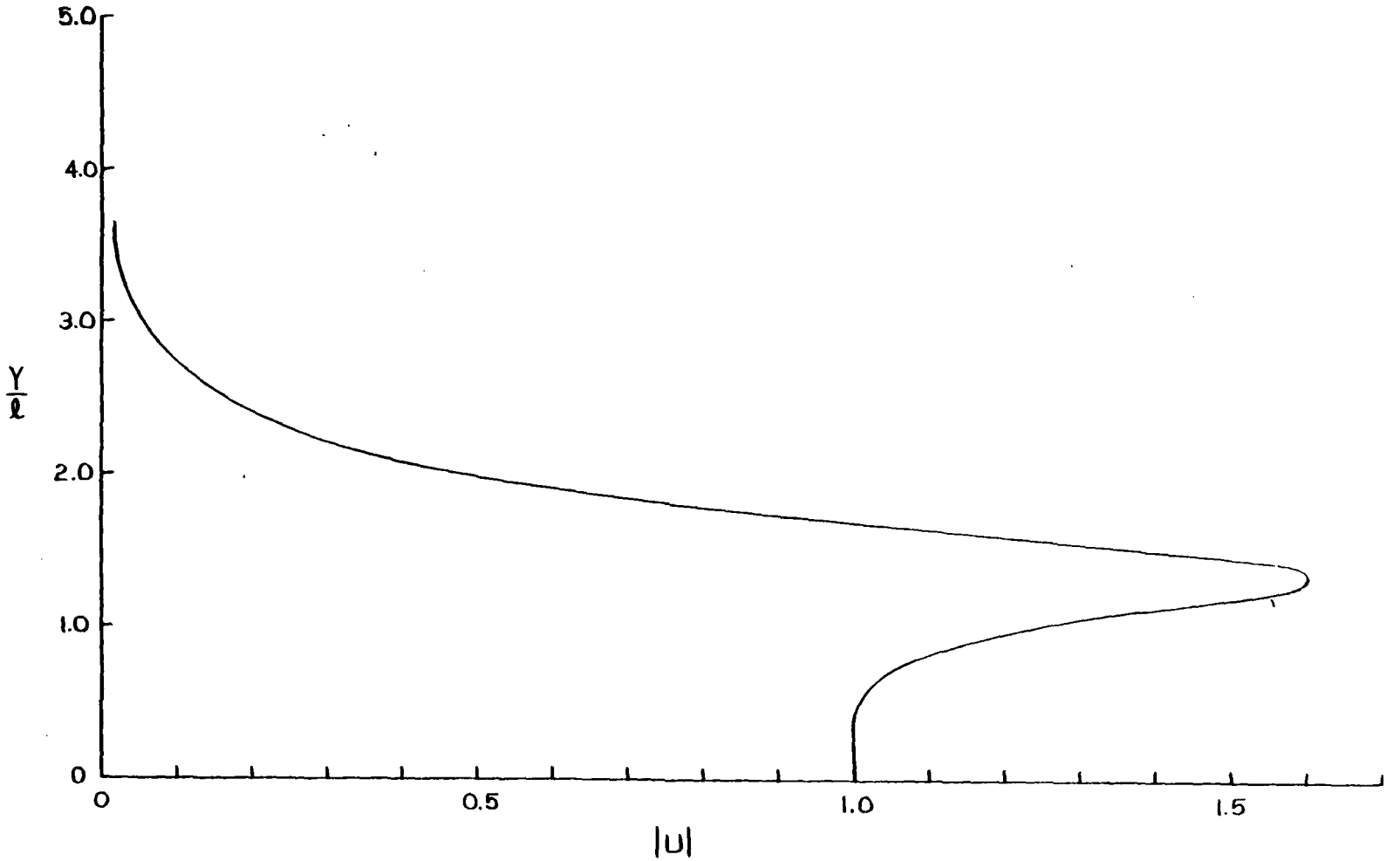

FIG. A-6 – PARTICLE DISPLACEMENT DISTRIBUTION. $n=4, R=0.05, \Gamma=22$.

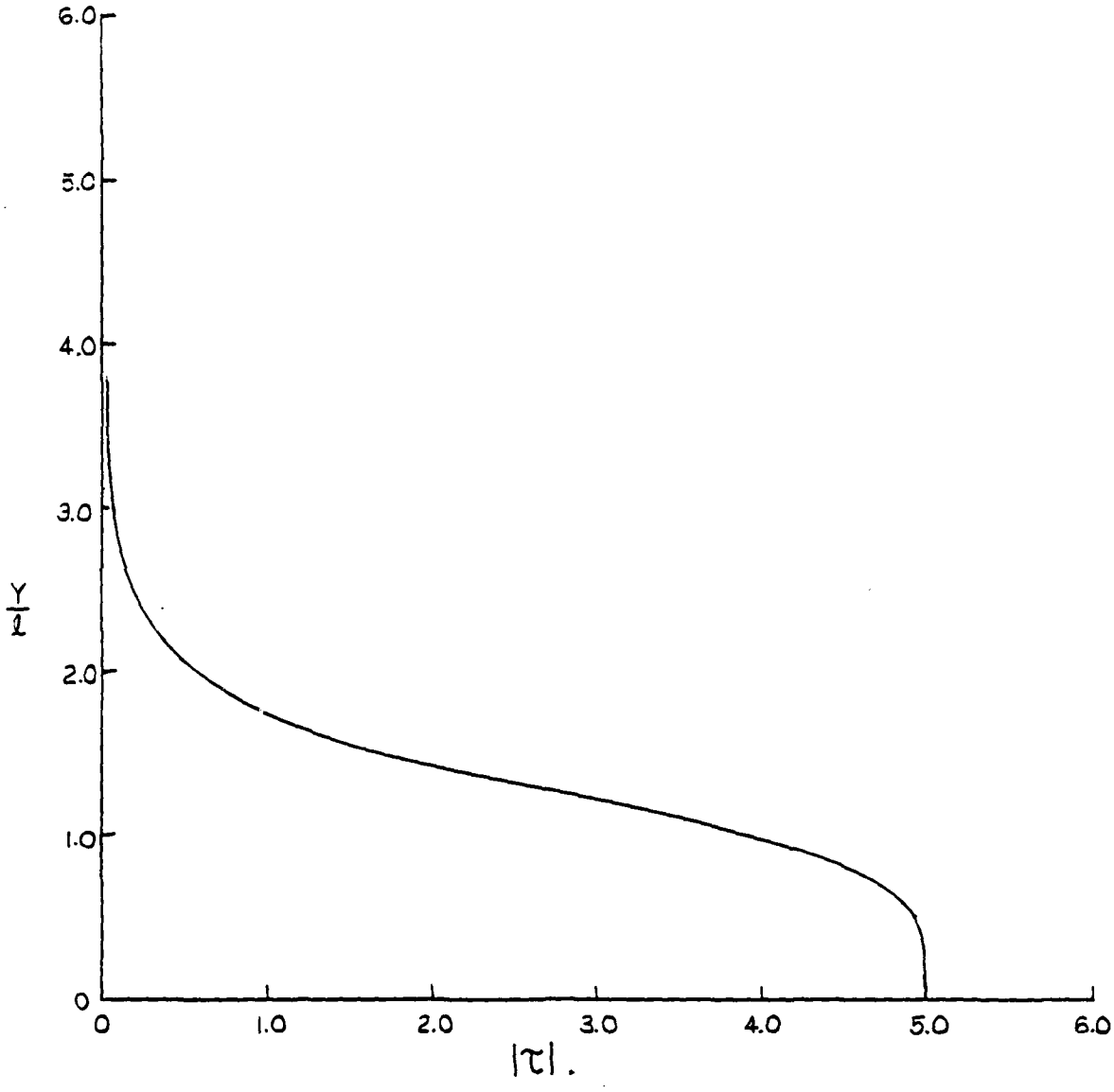

FIG. A-7 – SHEAR STRESS DISTRIBUTION. $n=4$, $R=0.05$, $\Gamma=22$.


DATE
FILMED
8-8